Materials Research Express

ACCEPTED MANUSCRIPT

Flexible piezoelectric energy generators based on P(VDF-TrFE) nanofibers

To cite this article before publication: Seung-Rok Kim *et al* 2019 *Mater. Res. Express* in press https://doi.org/10.1088/2053-1591/ab1ee8

Manuscript version: Accepted Manuscript

Accepted Manuscript is “the version of the article accepted for publication including all changes made as a result of the peer review process, and which may also include the addition to the article by IOP Publishing of a header, an article ID, a cover sheet and/or an ‘Accepted Manuscript’ watermark, but excluding any other editing, typesetting or other changes made by IOP Publishing and/or its licensors”

This Accepted Manuscript is **© 2019 IOP Publishing Ltd**.

During the embargo period (the 12 month period from the publication of the Version of Record of this article), the Accepted Manuscript is fully protected by copyright and cannot be reused or reposted elsewhere.
As the Version of Record of this article is going to be / has been published on a subscription basis, this Accepted Manuscript is available for reuse under a CC BY-NC-ND 3.0 licence after the 12 month embargo period.

After the embargo period, everyone is permitted to use copy and redistribute this article for non-commercial purposes only, provided that they adhere to all the terms of the licence https://creativecommons.org/licences/by-nc-nd/3.0

Although reasonable endeavours have been taken to obtain all necessary permissions from third parties to include their copyrighted content within this article, their full citation and copyright line may not be present in this Accepted Manuscript version. Before using any content from this article, please refer to the Version of Record on IOPscience once published for full citation and copyright details, as permissions will likely be required. All third party content is fully copyright protected, unless specifically stated otherwise in the figure caption in the Version of Record.

View the article online for updates and enhancements.

This content was downloaded from IP address 128.151.10.35 on 09/05/2019 at 23:53

IOP Publishing Smart Materials and Structures
Journal **XX** (XXXX) XXXXXX https://doi.org/XXXX/XXXX

Flexible Piezoelectric Energy Generators based on P(VDF-TrFE) Nanofibers

Seung-Rok Kim*, Ju-Hyun Yoo, Yong Soo Cho, and Jin-Woo Park**

Department of Materials Science and Engineering, Yonsei University, Seoul 03722, Korea

E-mail: jwpark09@yonsei.ac.kr

Received xxxxxx
Accepted for publication xxxxxx
Published xxxxxx

Abstract

Developing flexible/stretchable piezoelectric nanogenerators (PNGs) for powering various portable wearable electronic devices has attracted considerable attention. In this study, we investigate the effects of changing the degree of alignment and thermal annealing conditions on the mechanical properties and the performances of the polymer nanofiber PNGs. PNGs are fabricated with electrospun poly(vinylidenefluoride-cotrifluoroethylene) (P(VDF-TrFE)) nanofibers under various rolling and thermal annealing posttreatment conditions. Thermal annealing increases both the ferroelectric phase and the modulus of the nanofibers, and geometrically aligned nanofibers show anisotropic changes in modulus, stiffer in parallel direction stretching. The performances of PNGs fabricated under various conditions are compared, and the mechanism by which the mechanical properties are affected by the degree of alignment and thermal annealing is analyzed and discussed. The well-aligned and thermally treated PNG cells showed the increased power density value of 1.35 mW/cm^3 which is twice of the pristine randomly oriented samples without thermal treatment. Also, the nanofibers maintained its alignment structure after 10,000 times cyclic 7% stretching test without any cracks.

Keywords: P(VDF-TrFE), piezoelectric, nanogenerator, bending test, flexibility

*,** These authors contributed equally to this work.

1. Introduction

Flexible and wearable electronics are an emerging class of electronics that enable a wide range of applications, such as electronic skins, implantable devices, robotics, and prosthetics.[1, 2] Hence, the development of flexible power sources for such devices is in high demand given the possibility of harvesting energy from the environment in which the device is deployed.[1, 3] Piezoelectric nanogenerators (PNGs) are a promising technology for converting mechanical energy into electricity to drive various portable electronic devices.[3] Generally, the electrical output performance of PNGs is enhanced by electrical poling or annealing treatment, which involves high-voltage and high-temperature techniques.[4]

In the case of PNGs, inorganic ceramic piezoelectric materials such as lead zirconium titanate (PZT) and zinc oxide have been thoroughly studied due to their high piezoelectric coefficients (d_{ij}).[5] Ceramic-based PNGs, however, are limited by their rigidity and fragility and, in general, are unsuitable for continuous application, particularly under prolonged and/or extreme mechanical conditions.[5] Instead, piezoelectric polymers, some of which are ferroelectric and show significant piezoelectric properties, particularly at the nanoscale, such as polyvinylidene fluoride (PVDF) and its copolymers, as well as certain polyamides (nylons) in the appropriate crystalline phase, are prime candidates for PNGs that are flexible, robust, light, cheap, and biocompatible.[3, 5] In contrast to the inherent brittleness of piezoelectric ceramics, piezoelectric polymers also

Accepted Manuscript

 © xxxx IOP Publishing Ltd

demonstrate great potential to achieve flexibility and stretchability.[6]

Piezoelectric polymers, such as polyvinylidene fluoride (PVDF) and its copolymers, have been found to possess good piezoelectric properties.[7] PVDF consists of a carbon backbone with each carbon in the chain alternatively bound to two fluorine or two hydrogen atoms, oriented on opposite sides of the carbon chain.[3] The piezoelectric properties of PVDF arise from the larger difference in electronegativity between fluorine and carbon atoms than that between hydrogen and carbon atoms. Within a larger polymer structure, the dipole moments may sum to give a net electric dipole moment, depending on the crystalline geometry.[5, 8]

Typical thin-film fabrication often results in α-phase PVDF, which does not exhibit piezoelectricity due to the net cancellation of dipoles along the chain. Poling with either mechanical stretching, an electric field or controlled growth may force the polymer into a ferroelectric polar β-phase, which exhibits the strongest piezoelectricity.[6] Copolymers of PVDF where some of the hydrogen atoms are replaced with fluorine atoms are more likely to crystallize in a polar phase due to steric factors. Nevertheless, it has been reported that electrically poled poly(vinylidenefluoride-co-trifluoroethylene) (P(VDF-TrFE)) nanowire arrays can have a piezoelectric coefficient over 10 times higher than that of normal P(VDF-TrFE) thin films undergoing the same treatment.[3, 6, 9]

More recently, nanofiber synthesis approaches using a nanoconfinement growth effect have been found to be more likely to result in so-called 'self-poled' β-phase nanowires.[10, 11] Electrospinning is a widely adopted nanofiber synthesis method for a large selection of polymers. During the electrospinning process, the majority of polymer chains align along the axial direction of the nanofibers.[3, 6, 12] Since P(VDF-TrFE) is a linear polymer, the permanent dipoles are approximately perpendicular to the chain direction. Hence, in an electrospun nanofiber, the majority of the dipoles are aligned in the transverse direction with respect to the fiber axis.[6] In highly elongated nanofibers of P(VDF-TrFE), ordered crystallites are embedded within a highly ordered amorphous phase.[11] The percentage of the crystalline phase and the alignment of dipoles can affect the piezoelectric, ferroelectric, and mechanical properties of P(VDF-TrFE) polymer.[13, 14]

Despite numerous reports on PNGs composed of electrospun P(VDF-TrFE) nanofibers, there is a lack of deep understanding of the mechanical and piezoelectric properties of P(VDF-TrFE) nanofibers depending on the electrospinning conditions[3, 6] and the effect of this dependence on the performance of PNGs. In this study, we investigated the effect of electrospinning and thermal annealing posttreatment conditions on the degree of alignment of nanofibers and their mechanical and piezoelectric properties. PNGs were fabricated with nanofibers that were electrospun under various conditions, and the performances of the PNGs were tested and compared. Based on the test results, the mechanism by which the mechanical properties and the degree of alignment affect the performance of PNGs was analyzed and discussed.

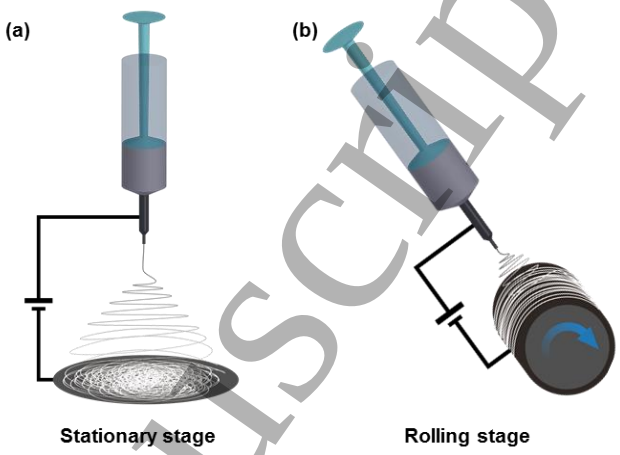

Figure 1. Schematic illustrations of the fabrication process of P(VDF-TrFE) nanowebs at the (a) stationary and (b) rolling stages.

2. Experimental section

2.1 Electrospinning

P(VDF-TrFE) (FC25 powder with a typical 25 mol % TrFE from Piezotech, France) solutions with powder concentrations of 10, 15, and 20 wt.% in a 3:2 weight ratio of DMF:acetone solvent were stirred at 200 rpm and 60 °C for 12 hours to achieve uniform solution dispersion. Electrospinning was performed using a system from NanoNC, Korea, at a high voltage of 8~9 kV with a flow pump feed rate of 4 μl/min. The distance between the electrospinning jet and collector was approximately 10 cm. The temperature was maintained at 20 °C, and the relative humidity was approximately 26%. To modify the geometrical alignment, nanofibers were spun for 1 hour onto a Si wafer surface (figure 1a, stationary stage for the 0 rpm sample) or Al foil (figure 1b, rolling stage for the 100, 200, and 400 rpm samples).

2.2 Thermal annealing

We chose 135 °C, which is higher than the Curie temperature (T_c) and below the melting temperature (T_m), as the annealing temperature. Annealing at this temperature is apt for the effective rearrangement of the polymer chain to form a more crystalline phase.[15] Additionally, the cooling process was controlled by varying the time for cooling; abrupt fast cooling was performed by placement on a metal

Accepted Manuscript

slab, and slow cooling was performed at a speed of 10 °C/min.

2.3 Characterizations

The morphologies of the P(VDF-TrFE) nanofibers were analyzed using field emission scanning electron microscopy (FE-SEM) (7610f-plus, JEOL Ltd.). The β-phase crystallinity was confirmed by high-resolution X-ray diffraction (HR-XRD) (SmartLab, Rigaku) analysis. The current and voltage generation were measured using a digital multimeter (DMM 6500, Tektronix).

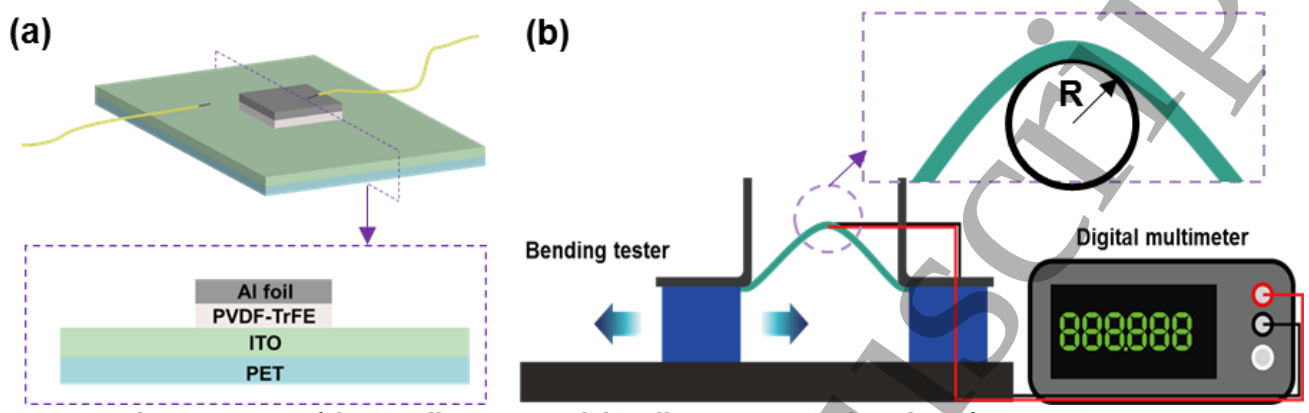

Figure 2. Schematic image of the (a) cell structure and (b) cell test set-up. (R: the radius of curvature)

2.4 Cell test

PNG cells were fabricated using random and aligned nanowebs (rolling speed of 400 rpm), as shown in figure 2a, and their performance upon cyclic bending (figure 2b, with 1.5 cm bending radius) was analyzed and compared. Figure 2a shows a schematic image of the cell structure. The layers of the cell consist of a commercial indium tin oxide (ITO)/polyethylene terephthalate (PET) substrate (purchased from Sigma-Aldrich, USA), electrospun P(VDF-TrFE), and an Al foil sheet. ITO and Al were used as charge-collecting electrodes connected to Cu wire. And all layered structures are anchored by Scotch tape. As shown in figure 2b, the cell detached to a bending tester was bent and its radius of curvature was 15 mm. Next to the bending tester, a digital multimeter (DMM) was connected to the cell to measure the generated current.

3. Results and discussion

As shown in figure 3, the thermal behavior of P(VDF-TrFE) powders was characterized via differential scanning calorimetry (DSC). The T_c' upon cooling, T_c upon heating, solidification temperature (T_s), and T_m of the powders were obtained as 68 °C, 100 °C, 126 °C, and 147 °C, respectively. Because T_c is the point of transformation from the ferroelectric phase to the paraelectric phase,[16] we chose 135 °C, which is higher than T_c and below T_m, as the annealing temperature. Annealing at this temperature is apt for the effective rearrangement of polymer chains, forming a more crystalline phase.[15] Additionally, the cooling process was controlled by varying the cooling rate: 1) fast cooling was performed by placing the sample on a metal slab, and 2) slow cooling was performed at a speed of 10 °C/min.

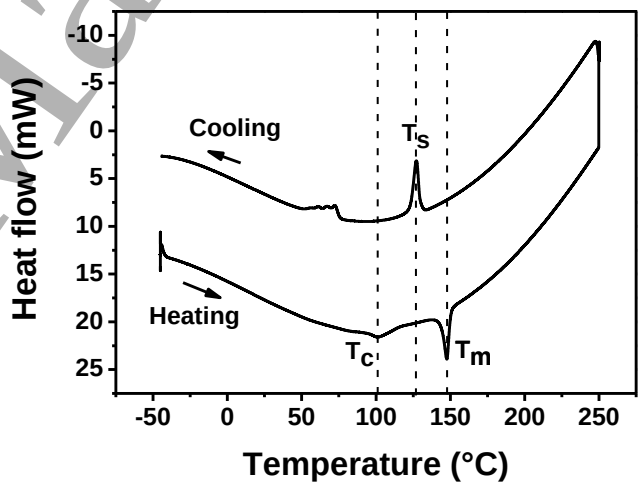

Figure 3. The DSC response of P(VDF-TrFE) powders. (T_c': Curie temperature, T_s: solidification temperature, T_m: melting temperature)

Figure 4 shows the electrospun nanofibers with different P(VDF-TrFE) powder concentrations. Nanofibers with a smaller diameter make denser nanowebs.[17] Hence, a lower concentration was expected to preferentially produce a smaller nanofiber diameter. However, as shown in figure 4, at 10 wt% P(VDF-TrFE), the lowest concentration, beads were formed along the nanofibers and on the webs. Therefore, a 15 wt% powder concentration was chosen based on the results in figure 4.

Accepted Manuscript

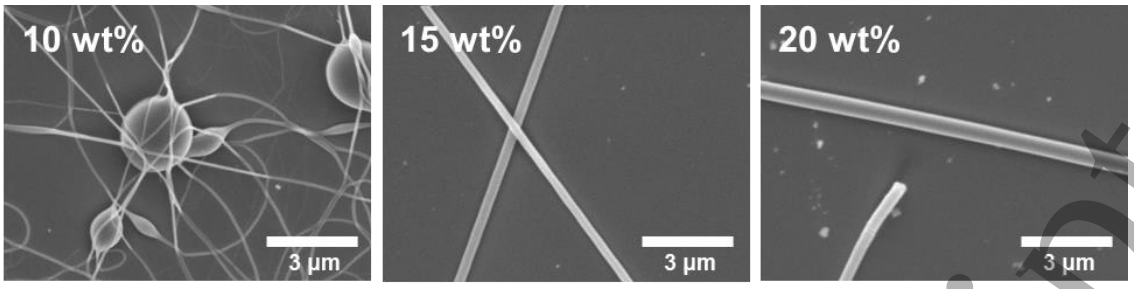

Figure 4. FE-SEM images of nanofibers with different concentrations of P(VDF-TrFE).

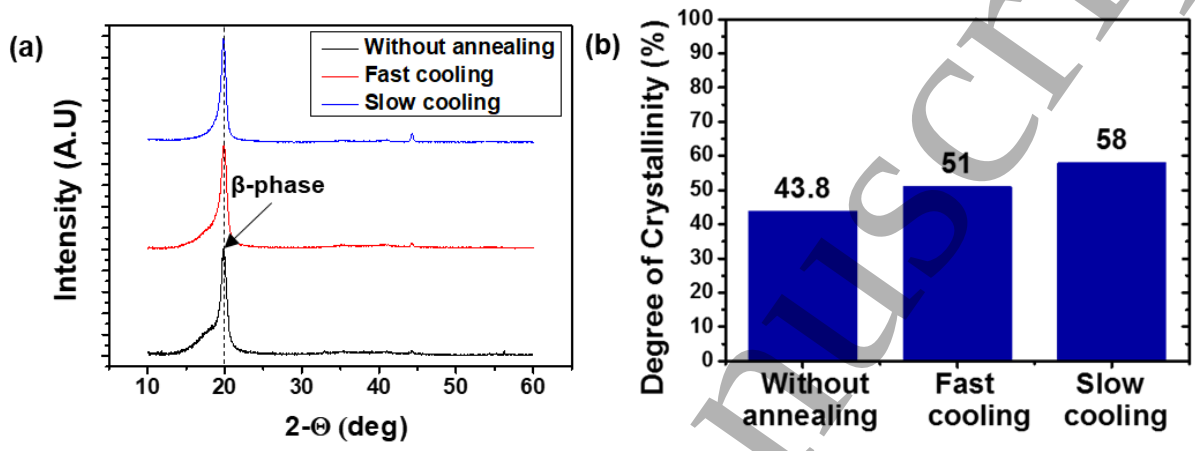

Figure 5. (a) HR-XRD analysis of P(VDF-TrFE) nanofibers with different annealing conditions and (b) the effect on the degree of crystallinity. The XRD patterns presented in (a) were normalized in relation to the β-phase peak intensity.

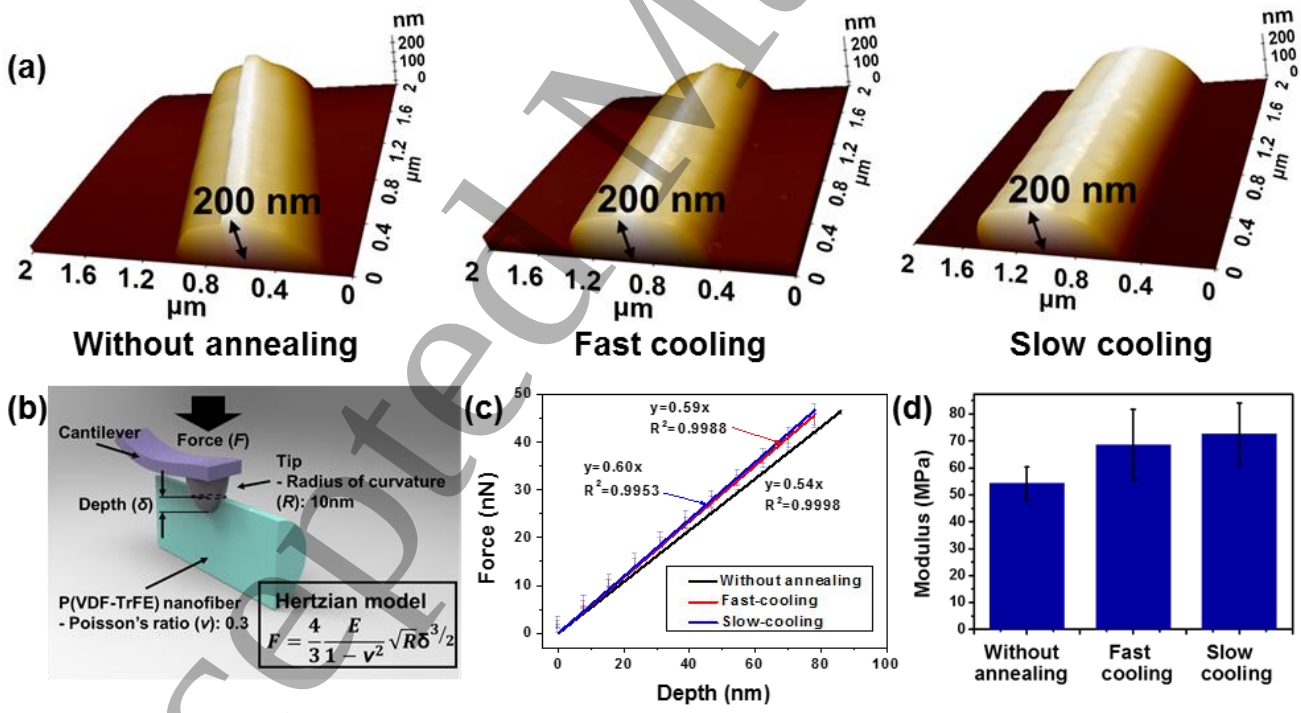

Figure 6. (a) AFM topography images of nanofibers with different concentrations of P(VDF-TrFE). (b) Schematic illustration of the nanoindentation method of measuring modulus using an AFM cantilever. (c) F-d curves of P(VDF-TrFE) nanofibers and (d) their modulus.

Accepted Manuscript

Because the ferroelectric β-phase exhibits the strongest piezoelectricity, the effects of the annealing and cooling processes on β-phase formation were investigated. The HR-XRD results (figure 5a) were used to determine the degree of crystalline β-phase in the electrospun nanoweb. We analyzed the diffraction peaks in figure 5a via the deconvolution method to fit individual peaks with Gaussian functions. The diffraction peak at a 2θ value of 19.9° corresponds to the (110)/(200) reflection of the crystalline β-phase, and the other broad diffraction peak near 17° corresponds to an amorphous phase. To compare the relative proportion of β-phase, we integrated the areas under each peak and calculated the ratio of β-phase area to amorphous area under the two different (fast and slow) annealing and cooling conditions mentioned previously (figure 5b). According to figure 5b, without annealing, the degree of crystallinity was 43.8%. After 2 hours of annealing, the degree of crystallinity was enhanced to 51 and 58% under fast cooling and slow cooling conditions, respectively.

Usually, the electromechanical coupling factors decrease as Young's modulus increases with constant stress condition.[18] This is because the materials with lower modulus are easy to be deformed. However, with constant displacement condition, the modulus can also enhance the power of PNGs with layered structure cell.[19] Hence, the modulus of each nanofiber in figure 6 was measured by nanoindentation. As shown in figure 6a, the annealing and cooling processes have no effect on the size of nanofibers (a 200 nm diameter was maintained). In figure 6b, we schematically illustrate the process of nanoindentation of a single nanofiber via the atomic force microscopy (AFM) cantilever. The tip of the cantilever pressed the surface of a nanofiber, and the cantilever body was deflected, measuring the force and the depth of the indented point. The radius of curvature of the parabolic tip was 10 nm, and we assumed that the deformation of a single P(VDF-TrFE) nanofiber corresponds to the Hertzian model[20] with a Poisson's ratio of 0.3. Figure 6c shows the force-distance (F-d) curves of each annealing and cooling process. With the Hertzian model, we converted the F-d curves to modulus values, as shown in figure 6d. According to the results in figure 6d, under slow cooling conditions, nanofibers become stiffer with an increasing degree of crystallinity.

Accepted Manuscript

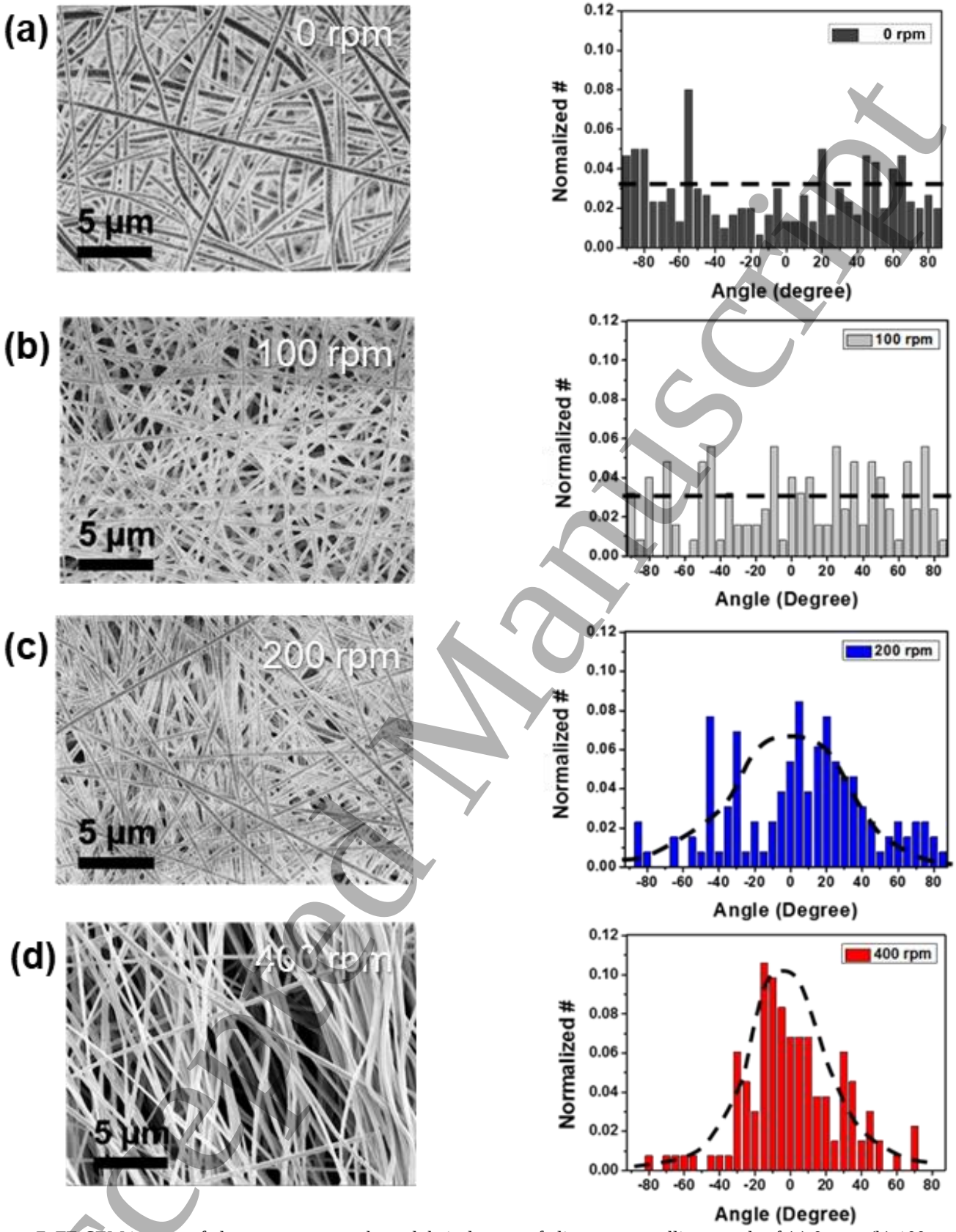

Figure 7. FE-SEM images of electrospun nanowebs and their degrees of alignment at rolling speeds of (a) 0 rpm, (b) 100 rpm, (c) 200 rpm, and (d) 400 rpm.

Accepted Manuscript

Controlling the geometrical alignment of nanofibers is also one of the most important methods for increasing the modulus of nanowebs to endow anisotropic properties along the biaxial stretching direction.[21] Figure 7 shows FE-SEM images and the degrees of alignment at different rolling speeds of 0, 100, 200, and 400 rpm. We counted the number of nanofibers every 5° along the slope in the FE-SEM images. For the quantitative comparison of the nanofiber orientation in relation to their electrospinning conditions, we calculated the standard deviations (SD) from the normalized number of nanofibers at every 5° angle range from the virtual vertical line (taken as the 0°) dividing the SEM images presented in figure 7. The mean normalized numbers of all the samples were about 0.2778. The 0, 100, 200, and 400 rpm samples showed SD values of 0.01539, 0.01758, 0.02392 and 0.03152, respectively. The 0 rpm sample showed the lowest SD value and thus, considered to have the most randomly oriented nanofibers. Consequently, although the 100 rpm sample had a very similar value of SD with that of the 0 rpm sample, the SD started to increase or the nanofiber orientation randomness began to decrease at this condition toward the increasing spin rate of the electrospinning roller stage. The angle of slope showed a sharper Gaussian distribution with increasing rolling speed, which clearly indicates that the nanofibers become more aligned with rolling speed.

To confirm that the rolling process is an effective method for aligning nanofibers, a tensile test was conducted to measure the modulus of the nanowebs. The material having the orientated networks usually shows different mechanical response to strain depending on stretching direction.[22] Aligned perpendicularly to the stretching direction simply spacing fibrils further apart, the nanowebs compensate the strain avoiding the breakage of each nanofiber. However, parallelly aligned nanowebs are spaced close to each nanofiber and positioned along stretching direction. This leads to direct mechanical response of the materials to the strain.[21, 23] Before the test, we defined stretching directions as 'parallel' and 'perpendicular' relative to the nanoweb alignment direction as shown in figure 8.

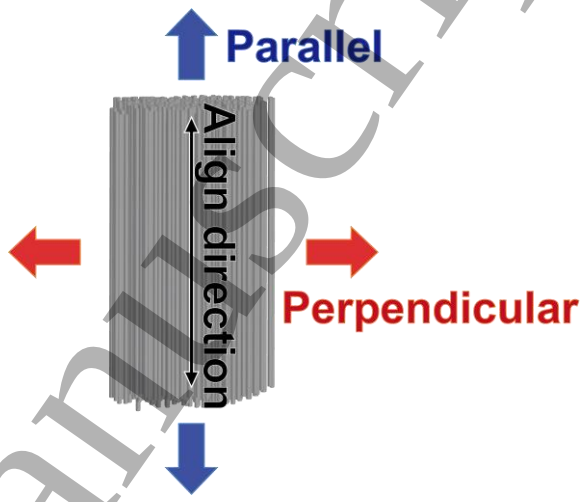

Figure 8. A schematic diagram for illustrating the stretching direction relative to the nanoweb alignment direction.

Accepted Manuscript

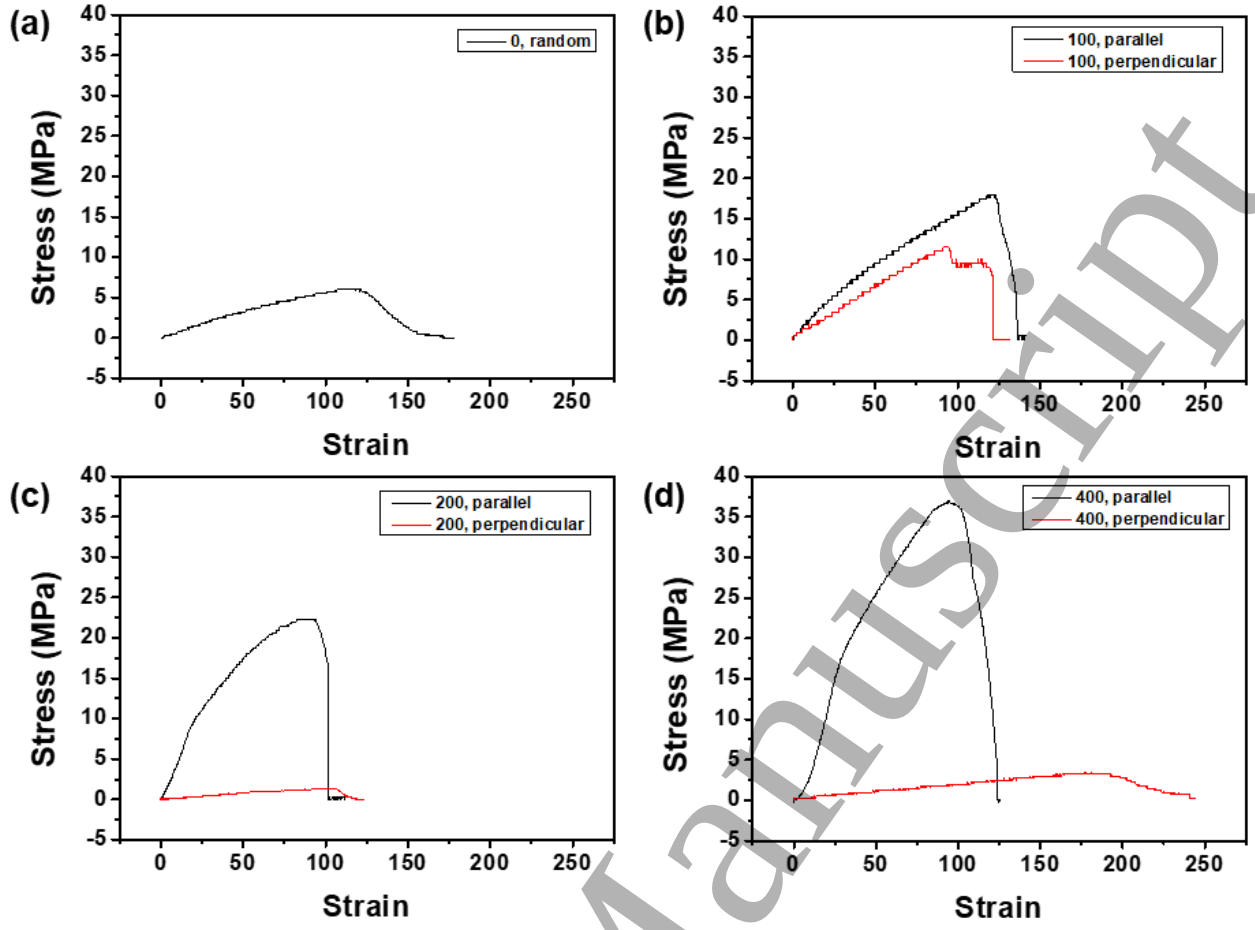

Figure 9. Tensile test results of electrospun nanowebs before thermal annealing fabricated at rolling speeds of (a) 0 rpm, (b) 100 rpm, (c) 200 rpm, and (d) 400 rpm with different alignment directions (parallel and perpendicular).

Accepted Manuscript

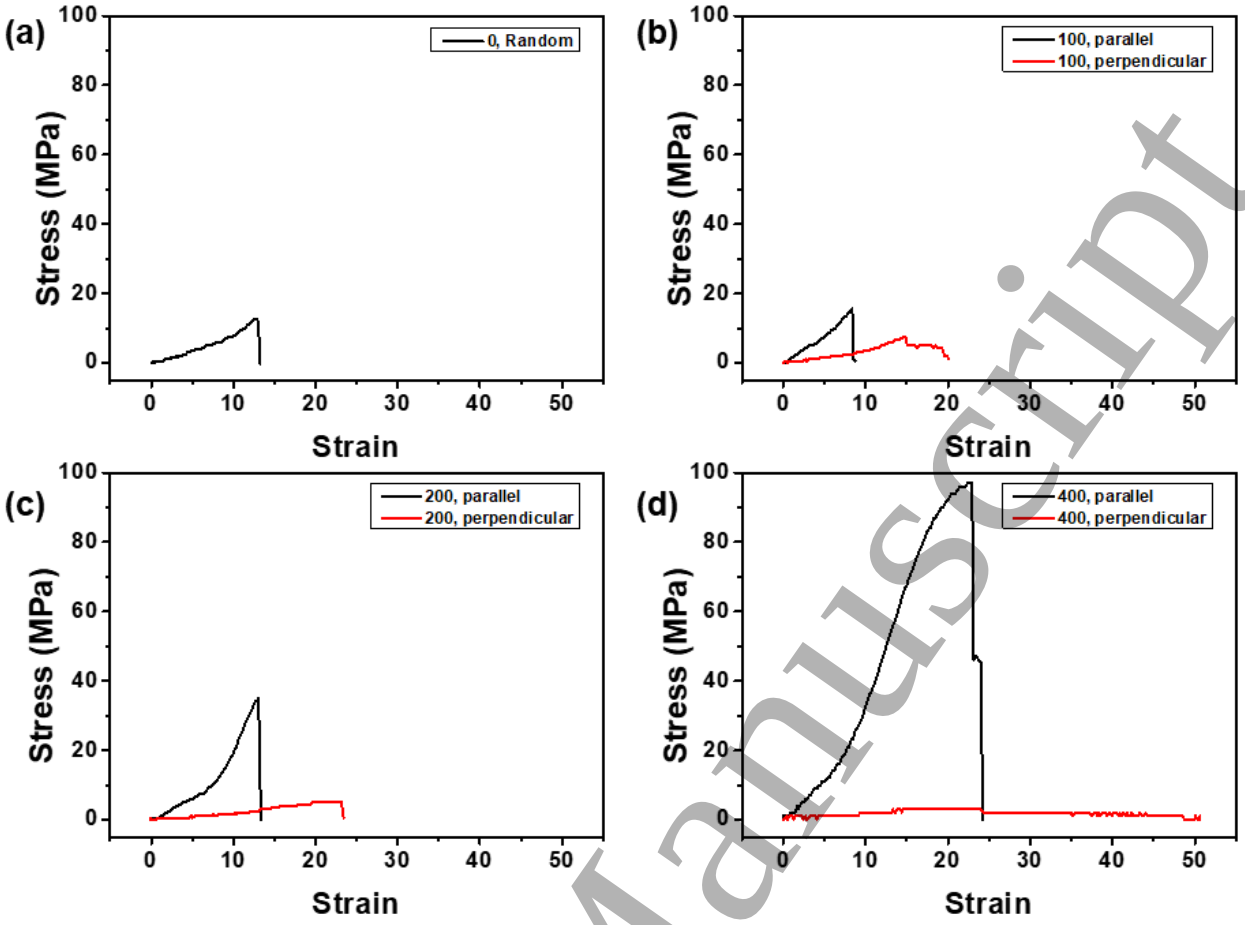

Figure 10. Tensile test results of electrospun nanowebs after thermal annealing fabricated at rolling speeds of (a) 0 rpm, (b) 100 rpm, (c) 200 rpm, and (d) 400 rpm with different alignment directions (parallel and perpendicular).

In figure 9, stress-strain curves of nanowebs fabricated at four different rolling speeds are compared. While the randomly oriented nanoweb had a modulus of 6.5 MPa, the moduli of the other nanowebs in parallel alignment increased with values of 19, 43, and 61 MPa and those in nanowebs in perpendicular alignment decreased with values of 13, 1.4, and 2 MPa at rolling speeds of 100 rpm, 200 rpm, and 400 rpm, respectively. As expected, the rolling stage made nanowebs aligned and the anisotropic stress-strain curves were obtained depending on stretching direction parallelly or perpendicularly.

After annealing and cooling process, mechanical tests were also performed on electrospun nanofiber mats for the various fabricating stage conditions. As mentioned previously in figure 6d, thermal annealing made the nanowebs stiffer regardless of the rolling speed. In figure 10a, the modulus of the randomly oriented nanoweb increased to 60 MPa with thermal annealing and slow cooling. This is 9 times stiffer values than the one without thermal treatment. Parallel stretching showed the increasing moduli values of 140, 200, and 330 MPa and perpendicular stretching showed the decreasing moduli values of 30, 15, and 10 at rolling speeds of 100, 200, and 400 rpm, respectively. (figure 10b-d) These moduli of the nanowebs with different rolling speeds also increased in both parallel and perpendicular direction stretching. Also, the ultimate tensile stresses were increased from the range of 5~40 MPa to 10~100 MPa after thermal treatment. Additionally, the fracture strain decreased from over 100% strain without thermal treatment to under 25% strain with thermal annealing.

Accepted Manuscript

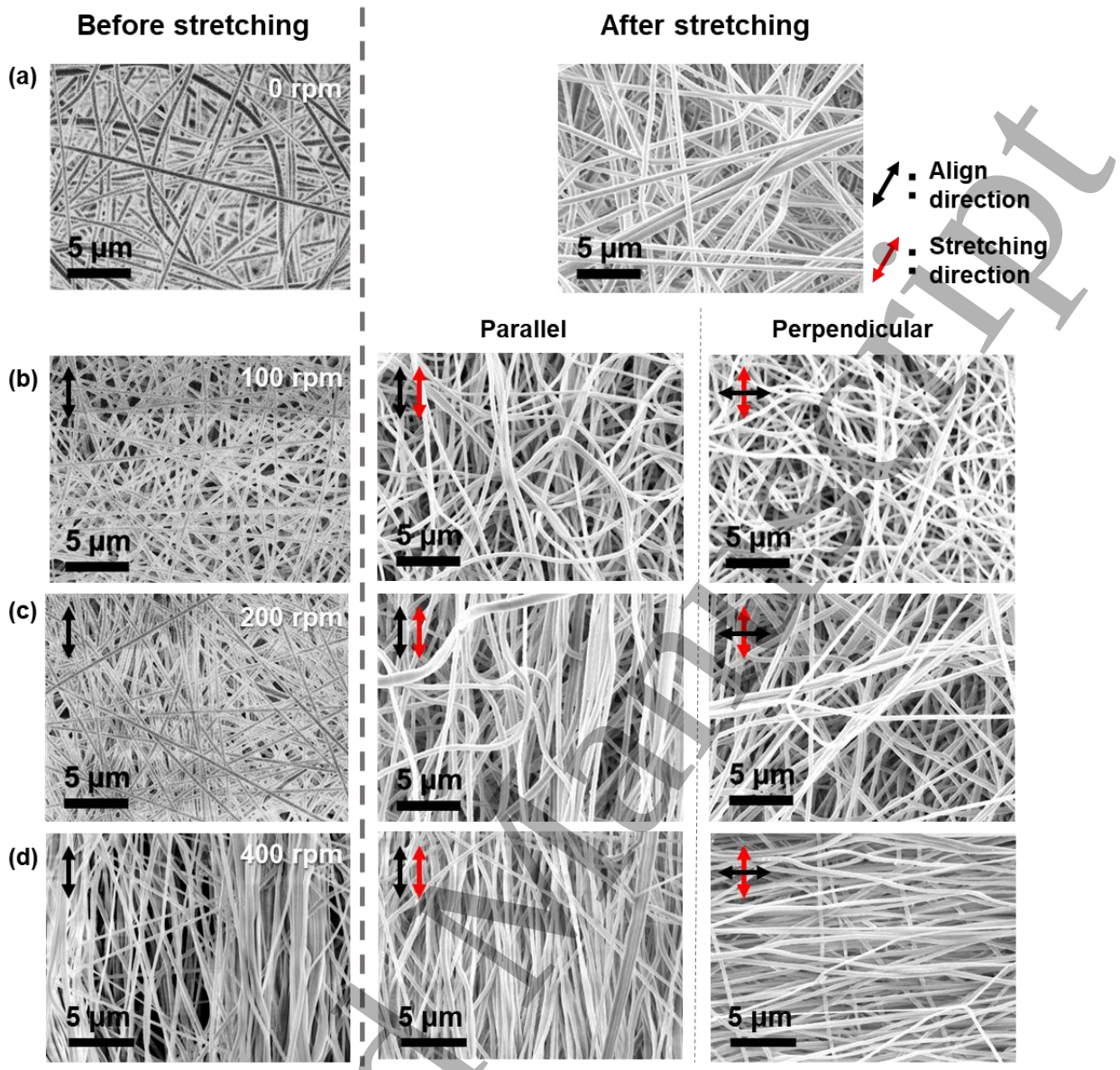

Figure 11. (a) FE-SEM images of before and after the cyclic tensile tests of nanowebs fabricated at the stationary stage. (0 rpm) Schematic diagrams of the stretching direction. FE-SEM images of the cyclic test results of nanowebs at rolling speeds of (b) 100 rpm, (c) 200 rpm, and (d) 400 rpm with different alignment directions (parallel and perpendicular to the stretching direction).

The FE-SEM images in figure 11 showed the structure of nanowebs with four different rolling speeds after 10,000 rounds of cyclic stretching at 7% strain. With the assumption that our full sample is 2 mm in thickness, 6.7% strain was expected to be applied to the cells while 15 mm bending. To test its anisotropic response to the strain, the cyclic strain was applied in two different-directions. We focused on both damages to the nanofibers and changes of alignment after stretching test.

There were no significant cracks or fractures inside the nanowebs after 10,000 cycles stretching test because 7% is not enough for the fractures as in figure 9. In the matter of the alignment change, while the stationary-stage sample showed little changes as in figure 11a, there were some loose nanofibers after stretching test in the samples fabricated at the rolling speed of 100 and 200 rpm (figure 11b and 11c). However, the samples with rolling speed 400 rpm showed little change in alignment and no loose nanofibers confirming the mechanical durability of the aligned nanofibers. This is because the strong attachments by the alignment among the nanofibers were maintained.[22] We could expect stable output performances with 400 rpm rolling stage sample.

Accepted Manuscript

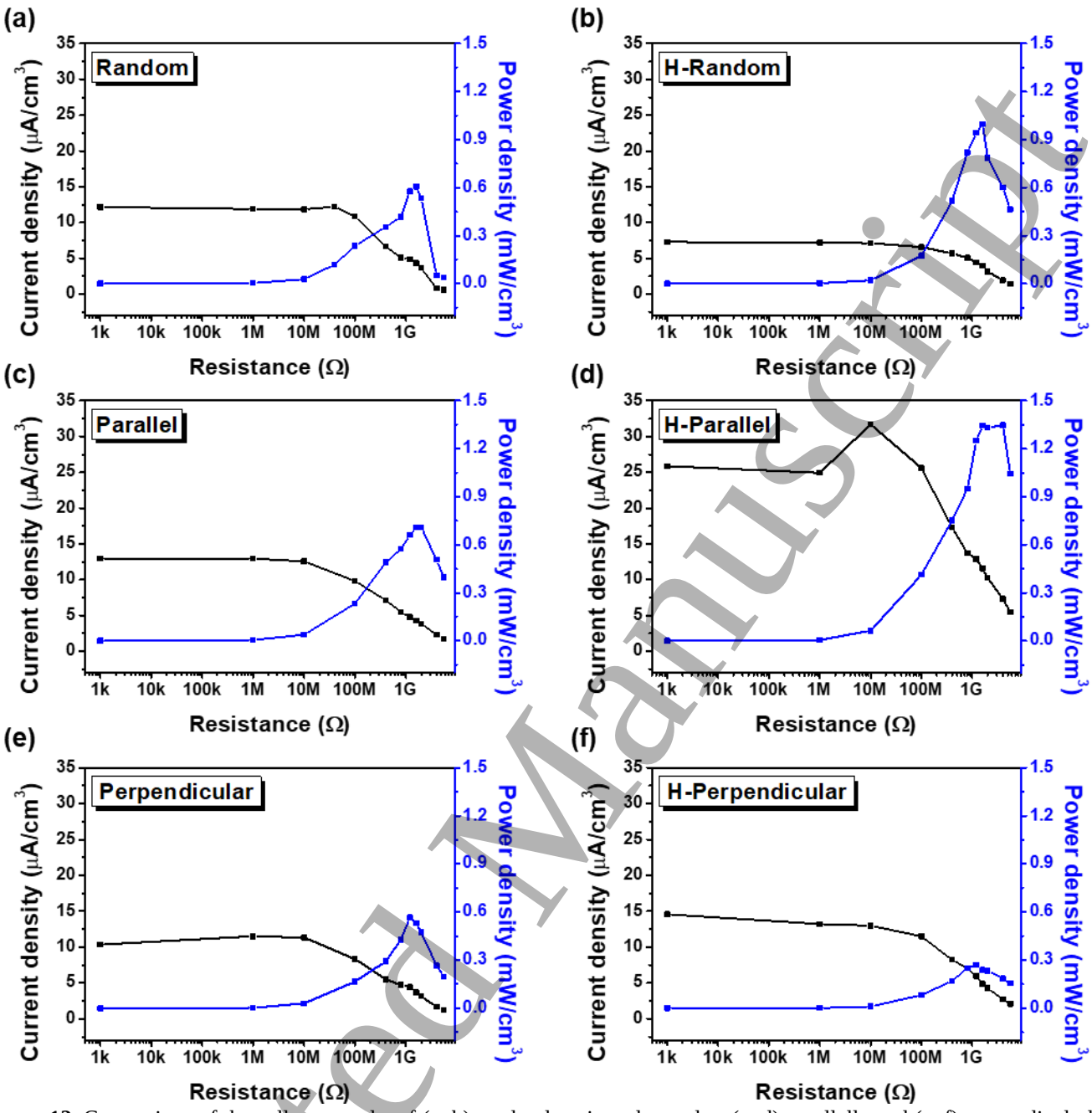

Figure 12. Comparison of the cell test results of (a, b) randomly oriented samples, (c, d) parallelly and (e, f) perpendicularly aligned samples produced at 400 rpm, (a, c, e) before and (b, d, f) after thermal annealing.

In figures 12, the performances of random and aligned PNG cells before and after thermal annealing are displayed. We designated the sample names as the stretching directions and the thermal annealing treatment with sign 'H-'. The cells were fabricated as the layered structure in figure 2a. We anchored full structures with Scotch tape to ensure the constant displacement while bending. And the bending test was also conducted with 15 mm bending radius of curvature.

Comparing the maximum power densities from figure 12a and 12b, the cells with thermally annealed and slow-cooled nanowebs showed 1 mW/cm^3 volume power density which is higher than 0.6 mW/cm^3 of the one without thermal annealing. Higher contents of the ferroelectric β-phase and stiffer property with constant displacement condition enabled higher output performances of PNGs.[10]

The performances of the geometrically aligned samples (the parallel and the perpendicular) showed a good correspondence to our tensile test results. Among the samples without annealing in figure 12a, 12c, and 12e, the maximum power densities of aligned samples changed

Accepted Manuscript

biaxially with the values of 0.71 mW/cm^3 for the parallel and 0.57 mW/cm^3 for the perpendicular. After thermal annealing in figure 12b, 12d and 12f, these output performances were diverged drastically with the values of 1.35 mW/cm^3 for the parallel and 0.27 mW/cm^3 for the perpendicular. By adopting both thermal and mechanical treatment, we could enhance the volume peak power density twice.

4. Conclusion.

We have studied the effects of thermal annealing and the geometrical alignment of nanofiber webs on the mechanical modulus change and their piezoelectric generation performances. Via XRD and nanoindentation analysis, we confirmed that thermal annealing not only improved the amount of the ferroelectric β-phase but also increased the modulus of the nanofibers from 6.5 MPa to 330 MPa. These higher crystal fraction and modulus contributed to the enhanced PNGs performances. Fabricated on the rolling stage, the geometrical alignments of nanofibers were conducted. Counting the oriented angles, we figured out that there were sharper Gaussian distributions with higher rolling speeds. Also, the geometrically aligned nanofibers fabricated on the rolling stage showed anisotropic changes in modulus, much stiffer in parallel direction stretching. Consequently, the piezoelectric energy generation performances were proportionally increased to the modulus changes after the thermal annealing and the alignment. The PNG cells fabricated at 400 rpm rolling stage and thermally treated showed the increased power density value 1.35 mW/cm^3 which is twice of the pristine randomly oriented sample. This is because of direct mechanical response to the parallel strain by narrowly spaced, aligned nanofibers. Also, the nanofibers maintained its alignment after 10,000 times cyclic stretching test without any cracks.

Acknowledgements

This research was supported by the Industrial Strategic Technology Development Program (#10079981) funded by the Ministry of Trade, Industry & Energy (MOTIE) of Korea and the Basic Science Research Program through the National Research Foundation of Korea (NRF) funded by the Ministry of Science, ICT & Future Planning (grant number: 2018R1A2B6001390).

References

[1] F. Yi, J. Wang, X. F. Wang, S. M. Niu, S. M. Li, Q. L. Liao, Y. L. Xu, Z. You, Y. Zhang and Z. L. Wang, 2016 ACS Nano **10** 7

[2] X. Wang, W.-Z. Song, M.-H. You, J. Zhang, M. Yu, Z. Fan, S. Ramakrishna and Y.-Z. Long, 2018 ACS Nano **12** 8

[3] M. Baniasadi, Z. Xu, S. Hong, M. Naraghi and M. M. Jolandan, 2016 Acs Applied Materials & Interfaces **8** 4

[4] B. Dudem, D. H. Kim, L. K. Bharat and J. S. Yu, 2018 Applied Energy **230**

[5] Q. S. Jing and S. Kar-Narayan, 2018 Journal of Physics D-Applied Physics **51** 30

[6] B. Zaarour, L. Zhu, C. Huang and X. Jin, 2019 Journal of Applied Polymer Science **136** 6

[7] B. Gusarov, Université Grenoble Alpes, 2015.

[8] J. Gregorio, Rinaldo and M. Cestari, 1994 Journal of Polymer Science Part B: Polymer Physics **32** 5

[9] J. Kim, J. H. Lee, H. Ryu, J.-H. Lee, U. Khan, H. Kim, S. S. Kwak and S.-W. Kim, 2017 Advanced Functional Materials **27** 22

[10] H. X. Li, T. Wu, M. H. Xie, Y. F. Shi, S. Shen, M. Zhao, X. Yang, L. M. Figueroa-Cosme, Q. F. Ke and Y. N. Xia, 2018 Journal of Materials Chemistry C **6** 38

[11] M.-C. García-Gutiérrez, A. Linares, I. Martín-Fabiani, J. J. Hernández, M. Soccio, D. R. Rueda, T. A. Ezquerra and M. Reynolds, 2013 Nanoscale **5** 13

[12] S. Ramakrishna, *An introduction to electrospinning and nanofibers*. (World Scientific, 2005).

[13] S. K. Ghosh and D. Mandal, 2018 Nano Energy **53**

[14] V. Strashilov, G. Alexieva, B. Vincent, V. S. Nguyen and D. Rouxel, 2015 Applied Physics A **118** 4

[15] M. W. Mohamad Hafiz, M. D. Rozana, S. Siti Zaleha, A. Adillah Nurashikin, S. Muhamad Naiman, M. Mohamad Rusop, G. Wee Chen and A. M. Wan Haliza, in *Advanced Materials Research* (2013), Vol. 812, pp. 60-65.

[16] D. E. Septiyani Arifin and J. J. Ruan, 2018 IOP Conference Series: Materials Science and Engineering **299**

[17] R. A. Abuzade, A. Zadhoush and A. A. Gharehaghaji, 2012 Journal of Applied Polymer Science **126** 1

[18] T. Ogawa, in *Ferroelectric materials-Synthesis and characterization* (IntechOpen, 2015).

[19] C. Baur, D. J. Apo, D. Maurya, S. Priya and W. Voit, presented at the ACS Symp. Ser, 2014 (unpublished).

[20] C. A. Schuh, 2006 Materials Today **9** 5

[21] J. Yao, C. Bastiaansen and T. Peijs, 2014 Fibers **2** 2

[22] M. Shin, J. Y. Oh, K.-E. Byun, Y.-J. Lee, B. Kim, H.-K. Baik, J.-J. Park and U. Jeong, 2015 Advanced Materials **27** 7

[23] J. Onorato, V. Pakhnyuk and C. K. Luscombe, 2016 Polymer Journal **49**

Accepted Manuscript